Proceedings of the ASME Turbo Expo 2018: Turbomachinery Technical Conference and Exposition
GT2018
June 11-25, 2018, Lillestrom (Oslo), Norway

GT2018-75861

AERODYNAMIC CONCEPTUAL DESIGN OF BOUNDARY LAYER INGESTION PROPULSOR SYSTEMS: A QUASI-2D THROUGH FLOW ANALYSIS METHOD AND MULTI-FIDELITY PROPULSOR DESIGN FRAMEWORK

B.J. Lee
Vantage Partners, LLC
Turbomachinery and Turboelectric Systems Branch, NASA Glenn Research Center
Cleveland, OH, USA

May-Fun Liou
Inlet and Nozzle Branch
NASA Glenn Research Center
Cleveland, OH, USA

Meng-Sing Liou
Propulsion Division
NASA Glenn Research Center
Cleveland, OH, USA

ABSTRACT

A propulsor design framework for maximizing the benefits of boundary layer ingestion is presented. The performance of BLI is strongly affected by all propulsor components, including the boundary layer characteristics (displacement thickness and form factor) of the ingested boundary layer at the inlet, the radial loading charactersitcs of the fan and exit guide vane (EGV), the area contraction from inlet to nozzle, and flow expansion at the exhaust cone. A strategy and its associated multi-fidelity design framework are proposed for an efficient conceptual design of the BLI propulsor which inherently differs from the conventional engine. In the framework, a quasi-2D through flow model served as the underlying fidelity model is introduced to incorporate the radial effect of the boundary layer entering the propulsor. Multi-fidelity design work is conducted to maximize the predefined performance metrics. On top of this efficient quasi-2D model, computational fluid dynamics based 3-D propulsor models are implemented to refine and validate the design. A BLI propulsion system integrated with fuselage is designed to showcase the framework. The performance of the resulting BLI propulsor system is evaluated via body-force model in unstructured Reynolds-Averaged Navier-Stokes (RANS) CFD and improvement is presented.

NOMENCLATURE

η_p : propulsive efficiency
λ : quasi-normal angle
φ : the meridional angle
ε : numerical error in angle definition
β : relative flow angle in rotational frame
α : turning angle
ω : rotational angular velocity
A : area
AIP : Aerodynamic Interface Plane
c : chord length
R : radius in the cylindrical coordinate
MFR : mass flow rate
FPR : fan pressure ratio
m : meridional direction
M : momentum
n : normal direction to the meridional direction
N_c : corrected speed
PR : total Pressure Ratio (FPR : fan pressure ratio)
P_p : propulsive power
T : thrust
U : tangential velocity of rotor ($r\omega$)
W : work
W_c : corrected flow

Subscript
h : hub
des : design
s : shroud (tip)
w : wall

INTRODUCTION

Over last few decades, extensive efforts have been made to understand the benefits of the boundary layer ingestion (BLI) since it was introduced to aviation propulsion.[1] The efforts

include conceptual designs of whole propulsion systems[2], aerodynamic designs of inlet[3], propulsor[4], aero-mechanics studies of distortion-tolerant fan[5], and etc. Recently, NASA and UTRC conducted an inlet-propulsor test and presented several promising results[6]. Besides showing a benefit of fuel burn reduction, high stall margin and low possibility of flutter beyond the expectations were observed. In addition to test rig based studies, various aircraft concepts including tail-cone thruster (STARC-ABL)[7], double-bubble (D8)[8-9], and hybrid wing-body (N3-X)[10] types of aircrafts have been designed and analyzed to take advantage of the BLI.

The BLI propulsion system is strongly integrated with airframe, thus, it has been difficult to separate the thruster from other components, i.e., airframe, inlet, and nozzle flowpath[11] even at the conceptual design phase. This characteristics of the BLI entices the development of a new set of thruster system analysis and design tools. In the present paper, we carried out the aerodynamic design of electric fan propulsors which ingest a significant amount of boundary layer from the fuselage through a multi-fidelity design technique. The diffusion factor of fan and EGV, wake recovery factor, power saving coefficient and/or propulsive efficiency are considered simultaneously. The conventional 0-D and 1-D turbomachinery analysis tools adopted in the system level design sometimes mislead the fuselage and inlet designs because the averaged number based in both annulus and radial directions oversimplifies the momentum and energy profile effect.[12-13] Thus, an extension from the 1-D model to include radial variations of flow turning and pumping is essential to assess the benefits of the boundary layer ingested propulsion by evaluating the wake recovery factor and power saving coefficients[1]. However, any increase of model fidelity would incur higher computational cost in optimization. As a result, we are proposing a simplified 2-D meridional through-flow method, referred here as quasi-2D model. It uses **net-work profile design** and **sequential sweep techniques of mass/area equilibrium along quasi-normal stations** to achieve a reasonable accuracy in predicting the flow turning, pressure ratio profiles, and efficiency. The area radial equilibrium is analytically solved in a conservative form of the momentum equation at each quasi-normal stations. The method avoids the numerical instability of conventional stream curvature methods by replacing meridional streamline re-construction. A whole fan-EGV (Exit Guide Vane) system model could be analyzed in seconds on a PC unit. Thus, a quick turnaround in obtaining appropriate turning of fan and EGV systems could be realized. The designed geometry is applied to body-force models in 3D RANS CFD for the flowpath design; here a multi-stage 3-D RANS turbomachinery code APNASA[14] is used to evaluate the correction factors of body force model. Finally, a conceptual design of BLI propulsion systems together with the fuselage and inlet/nozzle is proposed.

BENEFITS OF BOUNDARY LAYER INGESTION

The performance benefit of the boundary layer ingestion stems from the low momentum flow into the inlet so that the required power relative to a thrust equivalent clean inlet propulsor (i.e. non-BLI propulsor) gets low. Smith represented the benefits through two major performance metrics, i.e., the reduction of power for same thrust by power saving coefficient and propulsive efficiency. He also named the form factor of ingested boundary layer, and the wake recovery factor are major critical factors to maximize the power saving and propulsive efficiency. In Ref. 1, he proved that higher form factor will realize more power saving due to a low ram drag. But in the airframe perspective, excessively high form factor which may cause flow separation at the inlet entrance will increase the drag and lower the pressure recovery of the inlet. Thus, Hall et al.[9] derived a power balance method to compromise benefit of drag reduction and power saving of propulsion system. In the present BLI study, the authors see a perspective that the existence of fan itself will not affect the potential flow field of fuselage as long as it pumps the ingested flow (FPR >1, without choking) and the incoming boundary layer profile doesn't incur separation. For a ducted propulsors, however, the flow blockage of nacelle does affect the upstream flow. Thus, the airframe and inlet can be decoupled from the rest of design domain in the BLI propulsor because no matter how fan works the design at AIP to the downstream will not affect the upstream design in case the nacelle thickness is constrained.

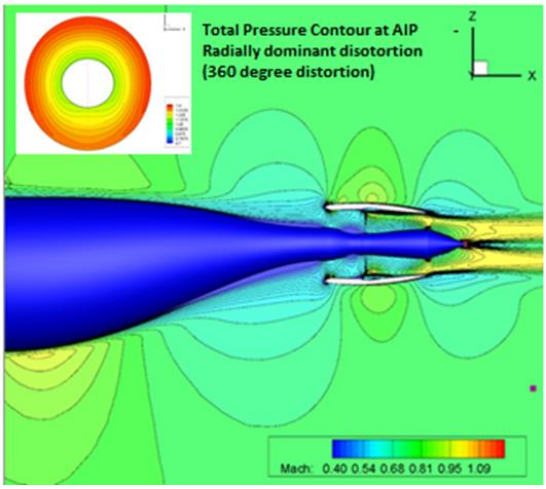

Figure 1. 3-D RANS CFD with body force model of the Tail Cone Thruster baseline design[19]. The inserted plot shows the circumferential total pressure contours at the fan face.

QUASI-2D THROUGH-FLOW MODEL

It is known that there are existing tools for analyzing/designing turbo-machinery propulsion systems, from low fidelity tool, like the 0-D empirical formulations to high fidelity for speed line analysis, 1-D or 2-D velocity vector models including stream-line curvature method, 3-D body force and full RANS turbo-machinery CFD models[12,13,14,15]. As mentioned above, there are three different BLI configurations currently being investigated under NASA Advanced Air Transportation Technologies BLI electric propulsion projects: tail-cone thruster (STARC-ABL)[7], double-bubble (D8)[8-9], and hybrid wing-body (N3-X)[10,11]. These concepts can be classified by the shape of distortion at fan face.

The embedded configurations, such as the N3-X and D8, have 180 degree-distortion entering inlet while tail-cone thruster is closer to 360 degree-distortion type[16]. The 360 degree distortion one has radially dominant distortion as shown in Fig. 1 while 180 degree-distortion type exhibits both circumferential and radial distortion as shown in Fig. 2.

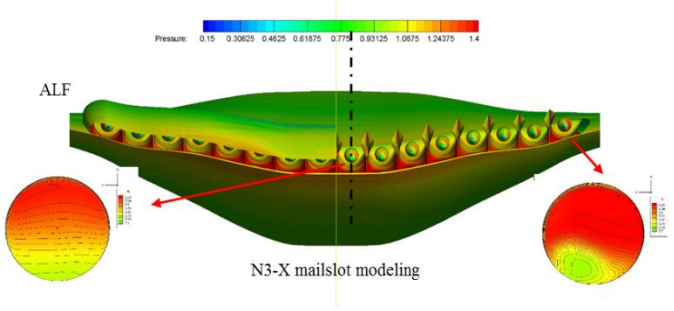

Figure 2. RANS CFD with body force model of the N3-X mailslot propulsors. Shown on the left is the total pressure contours of the first propulsor located from the center body symmetry plane as indicated by the black dotted line; on the right is the total pressure contours of the 8th propulsor.

In the turbo-machinery perspective, both distortions affect the fan operability and the performance critically. The present paper will address the radial distortion of ingested boundary layer. Most of the 2-D and higher fidelity models among mentioned tools have capability of designing fan and EGV but among them the stream-line (SL) curvature model sometimes suffers from convergence issue during the reconstruction process of stream lines in case with the existence of endwall defects. Thus, it has been difficult to utilize SL model in boundary layer ingestion model where the endwall profile is significantly weak. Here, a new quasi-2D through flow method which predicts stream-tube area of stream lines along quasi-normal with numerical robustness is suggested. It is devised to perform the velocity vector study of given internal flowpath, edge projection of blades and vanes, and inlet profile with radial distortion from CFD. Thus, the four key features of the model are (a) definition of quasi-normal along blade edge projection, (b) work profile design, (c) solution from qausi-normal, (d) radial momentum equilibrium equation in conservative form.

Each station in the fan/EGV flowpath is defined as shown in Figs. 3-(a) and (b). Figure 3-(a) shows the flowpath of the GE-R4 fan-EGV system.[17] The streamlines and flowpath are defined in a discrete manner on each quasi-normal station. Figure 3-(b) shows a streamline definition through the blade edge projection.

Physically, the meridional streamline will always pass the blade edge perpendicularly. Thus, in order to get rid of a source of numerical error in angle definition, ε, the meridional angle, φ, and quasi-normal angle, λ, are equated as in Eq. (1).

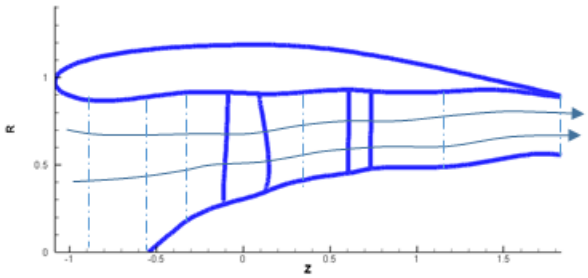

(a) Definition of quasi-normal stations in meridional view where R is the radius of the cone in a schematic GE-R4 fan-EGV system (cylindrical coordinate).

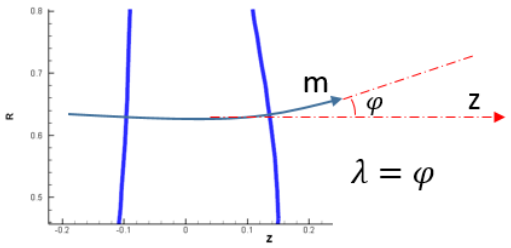

(b) The meridional direction of streamline through edge stations

Figure 3. Streamline and quasi-normal definition.

Thus, the differential operator along quasi-normal (y) and that along normal direction relative to meridional direction will be equated as given in Eq. (2). With this assumption, the $\frac{\partial \mathrm{M}_m}{\partial m}$ term in radial momentum equation which needs iterative calculation between different stations could be eliminated. Thus, radial equilibrium could be obtained without any other assumption in meridional differentiation for each quasi-normals.

$$\varepsilon = \phi - \lambda \sim 0 \quad (1)$$

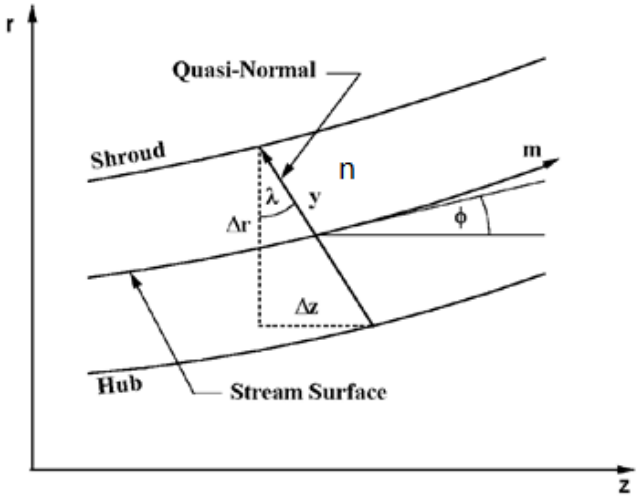

Figure 4. Quasi-normal angle and meridional angle definition at quasi-normal stations.[Ref. 13]

$$\frac{\partial}{\partial n} = \frac{1}{cos\varepsilon}\left[\frac{\partial}{\partial y} - sin\varepsilon\frac{\partial}{\partial m}\right] = \frac{\partial}{\partial y} \quad (2)$$

As a result, the radial momentum equation in a conservative form in Eq.(3) can be represented by Eq.(4) with time-steady, axi-symmetric assumption.

$$\frac{\partial \vec{M}}{\partial t} - \vec{W} \times (\vec{\nabla} \times \vec{M} + 2\rho\vec{\omega}) = \rho T \vec{\nabla} s - \rho \vec{\nabla} I \quad (3)$$

$$\frac{\partial M_m}{\partial y} + \left(k_m cos^2\beta + \frac{sin\beta - cos\beta}{r}\frac{\partial(rtan\beta)}{\partial y}\right) M_m + 2\rho cos\beta sin\beta\omega cos\varphi = \frac{\rho^2 cos^2\beta}{M_m}\left(\frac{\partial I}{\partial y} - T\frac{\partial s}{\partial y}\right) \quad (4)$$

Instead of traditional streamline reconstruction which causes numerical instability, solving the conservative form of the equation (14) provides a simple control of the area of each stream tube since each stream tube has constant mass flow rate.

$$M_m = \rho W_m = \frac{\Delta\dot{m}_i}{\Delta A_i}, \quad \text{thus} \quad \Delta A_i = \frac{\Delta\dot{m}_i}{M_m} \quad (5)$$

The procedures for the solution of equation (4) could be obtained by using a solution of non-linear ordinary differential equation with simple constraint of quasi-normal area for ducted flow.[13]

WORK PROFILE DESIGN

For a rotor design, a designer can choose the radial turning distribution depending on the stage reaction, fan pressure ratio and incoming flow. The most popular design is vortex free design which satisfies simple radial equilibrium equation in Eqs. (5) and (6).

The work per unit mass flow by a rotor is given by Eq.(6). The radial equilibrium equation in Eq. (7) drives the fact that the work required by a vortex free design is radially constant.

$$W = \Delta(UC_\theta) = \Delta(R\omega C_\theta) \quad (6)$$

$$\frac{dp}{dR} = \rho\frac{C_\theta^2}{R} \quad (7)$$

In order to achieve the desired work distribution, the rotor should work the sum of desired work as well as the profile loss. The profile loss of a drag force exerted on the blade is assumed to be proportional to R^3 as given in Eq.(8).

$$W_{loss} = \frac{F_{drag}U}{\dot{m}} = \frac{1}{2}\frac{\rho U^2 C_d U A_m}{\rho W_m A_\theta} \sim C_d R^3 \quad (8)$$

Thus, the required shaft work is a function of radius as in Eq.(8), see Fig 5.

$$W_{req} = W_{ideal} + W_{loss} = C_1 + C_2 C_d R^3 \quad (9)$$

where, $(C_d \sim loading, RC_\theta)$

If we adopt target polytropic efficiency in the radial function of work equation, (8),

$$W_{req}(r) = CpTt1\left((PR_{des})^{\frac{\gamma-1}{\gamma}} - 1\right) + C_{2'}r3 \quad (10)$$

where $C_{2'} = \frac{5}{2}CpTt1\frac{r_s^2 - r_h^2}{r_s^5 - r_h^5}\left((PR_{des})^{\frac{\gamma-1}{\gamma}} - (PR_{ideal})^{\frac{\gamma-1}{\gamma}}\right)$

and the design pressure ratio will be

$$PR_{des} = (TR)^{\frac{\gamma}{\gamma-1}\eta_p} \quad (11)$$

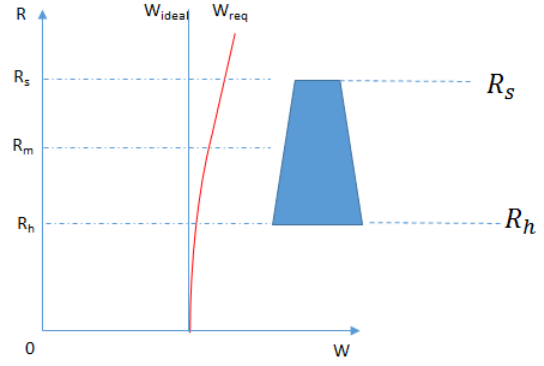

Figure 5. Required work profile and ideal vortex free work (Rs – tip radius, R_h – hub radius)

The function of radial work profile is imposed in the rothalpy calculation during quasi-2D model for the GE-R4 fan which is a traditional vortex free design. The turning angle predicted by quasi-2D model with design work profile is compared with RANS CFD[15] result at the 85%N_c in figure 6. The turning prediction looks reasonably close to the CFD profile as shown in the figure, and the total pressure and meridional Mach number prediction were observed in a good agreement with CFD profiles in Figs. 7 and 8.

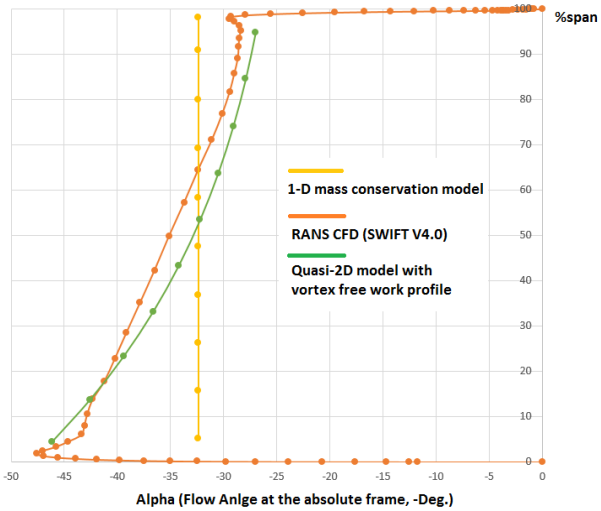

Figure 6. GE-R4 fan trailing edge, Turning prediction (-α, Deg.), at 85% N_c and W_c =93.6lbm/s.

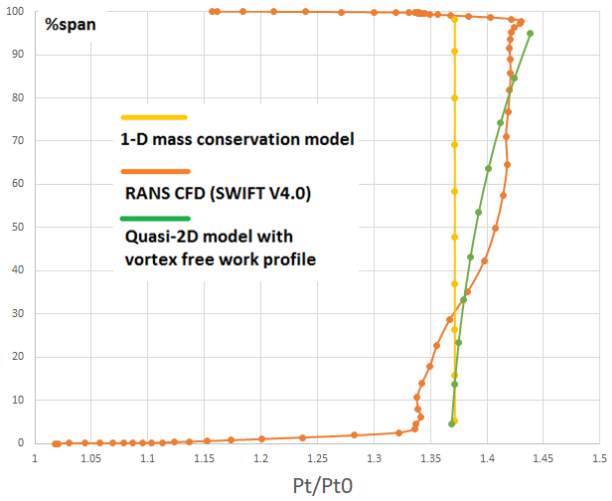

Figure 7. GE-R4 fan trailing edge, non-dimensional total pressure, at 85% N_c and W_c =93.6lbm/s.

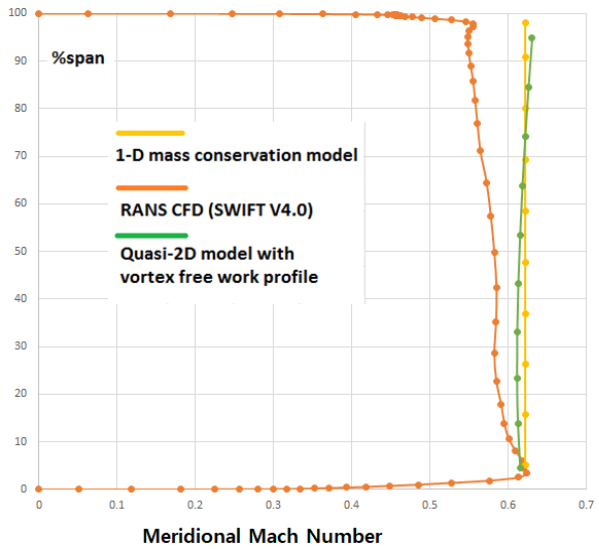

Figure 8. GE-R4 fan trailing edge, Meridional Mach number, at 85% N_c and W_c =93.6lbm/s.

LOSS MODELS AND BLADE GEOMETRY

Regarding loss models, Lieblein's design angle of attack (incidence), design deviation angle models[18] are used for obtaining metal angles out of the quasi-2D model. End-wall loss model is not applied in the model for now since the inlet profile already has massive low momentum flow from the boundary layer ingestion and the entrainment boundary layer well preserved through rotor stage to the EGV in a single stage model.

Since the model assumed the quasi-normal over a blade only at the edges, the meanline angle is assumed circular arc airfoil. Max thickness (t_m/c = 0.1) thickness distribution is following NACA65 series airfoil to leverage Lieblein models. A simple chocking condition ($M^2 < 1.1$) is applied to prevent choking through the flowpath.

MULTI-FIDELITY CONCEPTUAL DESIGN FRAMEWORK OF BOUNDARY LAYER INGESTION PROPULSOR

The conceptual design framework is as follows;

(1) To account for the radial profile of the ingested inflow, the boundary layer profile is acquired from CFD with 1-D mass flow boundary condition at the AIP.

(2) With the profile, corrected speed/flow (N_c, W_c) and given flowpath information, a quasi-2D model is constructed (input).

(3) The work profile is defined by designer's choice in the through flow model with constraint of diffusion factor. If there is an appropriate geometry tools, or if work profile can be manipulated by control points, an optimizer like NSGA-II[19] could be coupled and a full optimization work will be conducted. For the present work, the work and constraint are decided by designer's experience.

(4) Once the geometric definition of fan and EGV is obtained from low-fidelity analysis and design, the flowpath and blade/vanes are gridded with MMesh[14] and analyzed via APNASA to validate the flow turning angle prediction from quasi-2D and evaluate the correction factors for body-force model.

(5) With calculated correction factor, Goflow analysis is run with body-force defined by fan/EGV geometry, loss correction factors from low fidelity models. The flowpath is finally designed by investigating the wake recovery factor, propulsive efficiency, mass flow rate, and thrust.

CFD-BASED ANALYSIS AND FAN/EGV DESIGN

Once quasi-2D model finds appropriate geometry for a given boundary layer ingestion propulsor, the geometry is gridded and analyzed with APNASA on single passage model to derive radial correction factor and meridional entropy generation for body force model.

BODY-FORCE MODEL FOR PROPULSION-AIRFRAME-INTEGRATION

The body-force model[20,21] is a powerful method to evaluate the rotor and stator's performance and characteristics in 3-D RANS CFD modeling. The current body-force model of fan /EGV designs is implemented into Goflow code. Goflow is an unstructured mesh based 3-D RANS CFD solver with various turbulence models.[21] The body-force model applied in Goflow uses correction factors to represent the radial profile, speedline correction factors and metal blockage. Thus, the fan and EGV geometry designed from quasi-2D model is examined by a high fidelity CFD tool.

AIRFRAME/INLET INTEGRATION AND MODELING

The latest version of STARC_ABL fuselage is applied as a baseline of the present design.[7] The baseline fuselage and internal flowpath is shown in Figs. 9 and10. The design of

propulsor is focused on improving radial profile of fan to achieve required propulsive efficiency and the wake recovery factor with an assumption that AIP total pressure contour is preconditioned with low circumferential distortion (<2%). The airframe in the final configuration is designed by Gaetan et al.[22] with multi-point adjoint based design approach. The design conditions are at three different angle of attacks of 0°, 2°, 4° at freestream Mach number of 0.785. Reynolds number per unit length (meter) of the airframe is 5.67E+06. The reference length is the fuselage length of 38.1m. The fan design parameters are corrected flow W_c=636.2kg/sec, corrected speed N_c=2885 RPM, fan pressure ratio FPR =1.25 and angle of attack, AOA=2°. The form factor (H) of the airframe and inlet is 1.21, the DPCP (circumferential distortion) is 0.02. The mass flow captured by the baseline inlet is 138kg/sec at altitude of 11.3km (37k ft.). Figure 11 shows the total pressure contour at the AIP and the radial total pressure profiles entering the fan face. As mentioned above, the circumferential variation of fan-face profile is not as significant as radial's, thus, the design goal is to enhance the momentum at the hub with more pumping work as far as the diffusion factor allows.

Figure 9. Fuselage and propulsor of the baseline.[7]

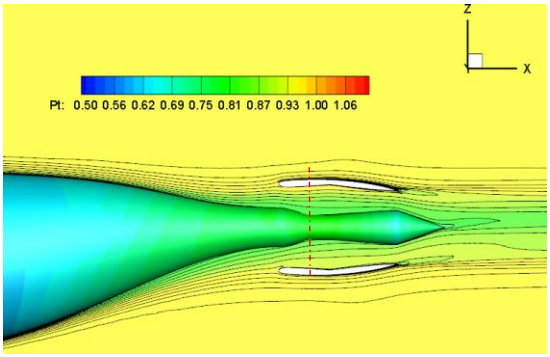

Figure 10. Boundary layer ingestion and flow through the baseline propulsor displayed in Pt/Pt_∞ contours at MFR=109kg/sec, and M_∞=0.785.

PERFORMANCE METRICS

The propulsor is designed based on multiple performance metrics which is introduced by Smith for BLI propulsor.[1] Most of all, the form factor (H) which is the ratio of wake momentum area (θ) to displacement area (δ) is used to describe the low momentum flow into the propulsor. He also introduced propulsive power (P_p) as given in Eq. (12)

$$P_p = \dot{m}\left(V_j^2/2 - V_0^2/2\right), \tag{12}$$

by adopting propulsive power, the propulsive efficiency can be represented by Eq. (13)

$$\eta_p = V_0 T/P_p, \tag{13}$$

where, T is thrust $(= \dot{m}(V_j - V_0))$, V_0 and V_j are the free-stream velocity and jet velocity respectively.

By introducing the ratio of propulsive power to actual shaft power which is denoted by η_{KE}, the overall propulsor efficiency, η, can be evaluated via Eq. (14).

$$\eta = \eta_p \eta_{KE} = V_0 T/P \tag{14}$$

where P is the actual shaft power.

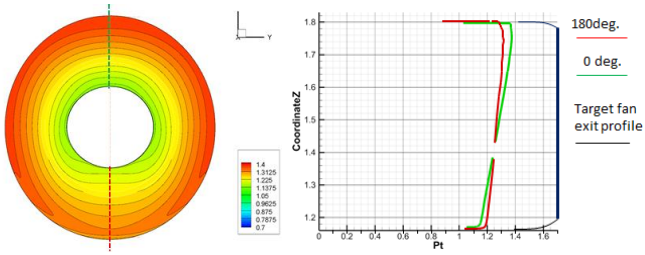

Figure 11. Total pressure contour [22] and profiles of the baseline airframe and target fan exit profile.

FAN/EGV DESIGN WITH FLOWPATH CONSIDERATION

The initial baseline flowpath is not turbo-machinery favorable as shown in Fig. 10. The shroud flowpath has divergence which will cause high diffusion factor at the rotor tip. In addition, the hub radius is constant throughout the fan hub, thus, hub flowpath contraction is needed. As the hub momentum is low, the design concept is to keep the hub area converging and the shroud area constant. To allow the hub contract as much as possible, a reduction of the camber of nacelle cowl is employed. Figure 12 shows quasi-2D domain of internal flowpath.

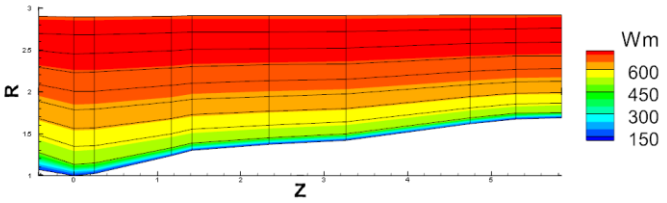

Figure 12. Flowpath design and boundary layer entrainment through quasi-2D model, where W_m is the meridional velocity (ft/sec).

As for fan design concepts, we have developed two different profile concepts as presented in Fig. 13. One is the conventional vortex free type fan (VF) and the other is hub strong profile fan (HSF). The fan exit total pressure profile of these two concepts are given for a same fan pressure ratio of FPR=1.25. The HSF provides exit profile closer to the target fan exit profile than the VF one.

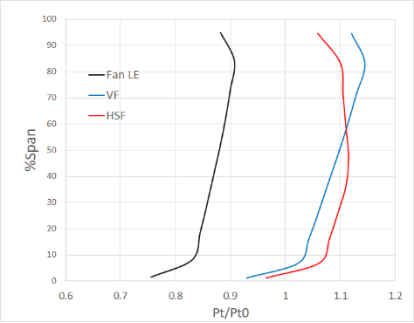

Figure 13. Conceptual Design of Fan Exit Pressure Profile

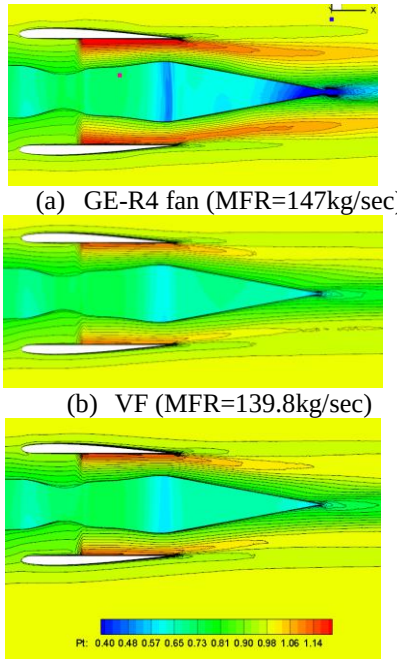

(a) GE-R4 fan (MFR=147kg/sec)

(b) VF (MFR=139.8kg/sec)

(c) HSF (MFR=140.6kg/sec)

Figure 14. Designed flowpath with (a) GE-R4 fan, (b) VF, and (c) HSF in RANS CFD analysis.(N= 2500RPM, altitude 37kft)

The fan design concepts obtained from quasi-2D model are applied to the flowpath with hub contraction and are compared with GE-R4 fan/EGV (design FPR=1.49) in the same flowpath at the same rotational speed (2500 RPM) in 3-D RANS CFD model in Fig.14. The HSF (design FPR=1.25) pumps more mass flow than what VF does. In addition, the total pressure contours in Figs. 14-(b) and (c) indicate that the jet from HSF is stronger than VF case. Table 1 presents the comparison of performance metrics of these three different fan/EGV configurations in the first type flowpath design. The HSF generates more thrust than VF but overall propulsor efficiency is slightly poorer. As the HSF fan works more at the hub region and pumps higher momentum flow through the nozzle throat, the expansion throughout nozzle and exhaust cone affects its overall propulsor efficiency remarkably. The form factor is measured at inlet highlight for the stream tube area which flows the same MFR as at the AIP.

Performance Metrics	GE-R4	VF	HSF
Form Factor	1.73	1.39	1.49
MFR (kg/sec)	147	139	141
Thrust (kN)	10.13	9.06	9.57
Propulsive power (kW)	1935.3	1658.5	1780.4
Shaft power (kW)	3407.7	2388.4	2627.0
Propulsive Efficiency	1.21	1.27	1.25
Propulsor Efficiency (%)	68.83	87.91	84.4

Table 1. Performance Comparison of fan/EGV configurations (Type 1 flowpath, 37,000 ft., N=2500 RPM)

EXHAUST CONE FOR WAKE RECOVERY

In the table 1, GE-R4 fan shows a massive loss from the nozzle and exhaust cone as it pumps more mass flow rate than other two new designs. HSF fan also showed slightly lower efficiency than VF fan due to same reason. The internal hub flowpath is slightly revised to lower the nozzle throat Mach number to be below 0.8 to prevent a lossy expansion at the downstream and wake. In addition, the exhaust cone is stretched to have benign expansion curve as shown in Figs. 15-(a) and (b). To distinguish this revised flowpath from the previous flowpath, this is named type 2 flowpath and the previous design hereafter is named type 1. Figs. 15 compares the Mach number contours of the HSF and VF in the type 2 flowpath with stretched exhaust cone. The HSF pumps more flow as higher momentum flow is observed at the nozzle throat and downstream jet. Also, the concave shaped exhaust cone limits the growth of low momentum/low Mach number area for both cases when compared with the type 1 shown in Figs 14-(b) and (c). Similar to the Table 1, Table 2 summarizes the performances of the VF and HSF coupled with the type 2 flowpath. Although the propulsive efficiency slightly reduced for both cases from Table 1, however, the shaft power is reduced and the loss through the nozzle is reduced as well. Table 2 shows the HSF has an overall +0.8pts.% increase on the propulsor efficiency from its counterpart in the Table 1 and a +0.2pts.% proplsor efficiency increase for the VF.

Performance Metrics	VF	HSF
Form Factor	1.83	1.80
MFR (kg/sec)	139	142
Thrust (kN)	9.22	9.57
Propulsive power (kW)	1691.2	1780.4
Shaft power (kW)	2422.8	2608.2
Propulsive Efficiency	1.26	1.24
Propulsor Efficiency (%)	88.1	85.2

Table 2. Performance Comparison of fan/EGV configurations (Type 2 flowpath, 37,000 ft., N=2500 RPM)

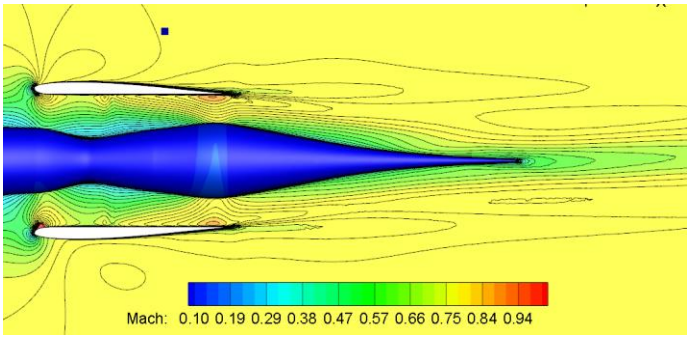

(a) HSF (MFR=142kg/sec)

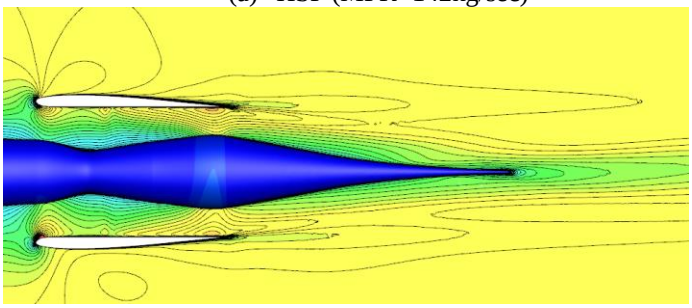

(b) VF (MFR=139kg/sec)

Figure 15. Designed flowpath with (a) HSF, (b) VF in RANS CFD analysis. (N= 2500RPM, altitude 37,000ft)

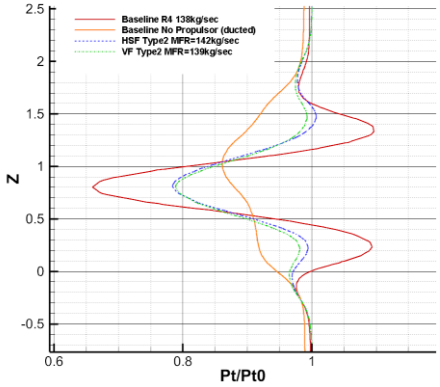

(a) Total Pressure Profiles

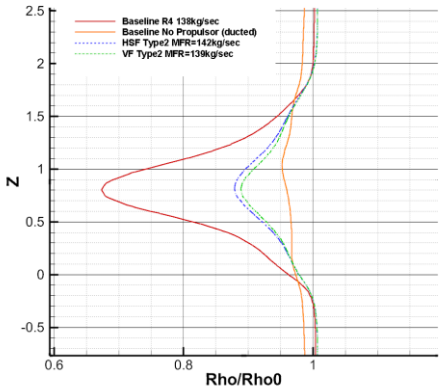

(b) Density Profiles

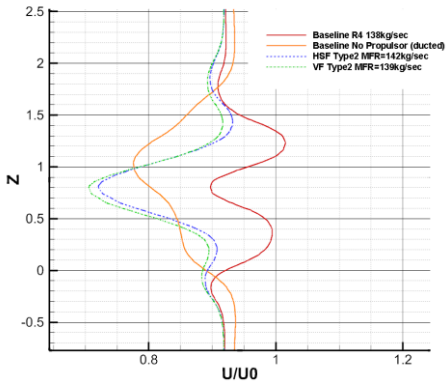

(c) Velocity Profiles

Figure 16. Wake profiles at x=42m which is 5.2m downstream of the nozzle throat (N= 2500RPM, altitude 37,000ft). Z=0.8192m is the center of engine rotation.

The wake profiles along z-direction for type 2 cases compared with baseline in Figs.16. R4 fan with baseline is presented as a reference. The wakes are measured at x=42m while nozzle throat locates at x=36.8m. Since the fan is designed higher pressure ratio, it generates higher thrust as shown in 16-(a). Both HSF, VF fans show benign pumping with less loss at the core flow. The density profiles in 16-(b) shows that new propulsor shapes pump more flow to the core. In addition, the mixing between high and low total pressure flow got much smaller as shown in 16-(a), thus, less loss is expected at the further downstream. Fig. 16-(c) compares the axial velocity profiles.

PERFORMANCE EVALUATION OF CONCEPTUAL DESIGN

In our final propulsion-airframe integration (PAI) study, type 2 propulsor with two different fan designs are integrated with the airframe designed by Gaetan et al.[22] by means of distortion minimization at multiple points. It is noted that current conceptual design work is based on a single point consideration, i.e. angle of attack of 2°. Their resulting optimized configuration has oval shaped fuselage and inlet which is not the least distortion shape for the angle of attack of 2°. The PAI performances are evaluated in Table 3. HSF pumps more flow, the same trend as already demonstrated in type 1 and 2 propulsors. HSF generates more thrust as well. However, the VF exhibits a much higher overall propulsor efficiency because the shaft power is about 10% lower in the VF case. Figure 17 shows the total pressure contour comparison between baseline airframe and distortion minimized airframe at the AIP. A higher total pressure region is observed along the y-direction in Fig. 17-(a) and results in tip distortion and more flow entrained to the tip of the VF. This phenomenon mitigates the aerodynamic degradation from the distortion caused by the oval shaped airframe. Figure 18 is the Mach contours in the x-z plane of both integrated configurations. The differences of fuselage shape is that the inlet throat area is extended so that more flow is ingested along x-z plane, while that in x-y plane is narrower. Thus, a

circumferential area variation mitigated drastic distortion change at different angle of attack conditions. When compared with Figs. 15 and this PAI study provides an evidence that upstream influence from fuselage affects the propulsor performance.

CONCLUSION

The present approach successfully demonstrated the accuracy and applicability of the proposed quasi-2D method for the design of a BLI propulsor. This paper addresses the method, multi-fidelity design framework and fan-EGV system designs for the BLI aircrafts. The propulsor of a tail-cone-thruster aircraft, STARC_ABL, is designed by the proposed conceptual design framework. The performance of two concepts of fan design, i.e., vortex free design (VF) and hub strong profile design (HSF) coupled with different flowpathes and nozzles are assessed and compared by the engine performance metrics. The HSF pumps more flow and generates more thrust in general. The propulsive and propulsor efficiencies, however, are better in VF cases about +3% for both type 1 and 2 propulsor designs. The multi-point distortion minimized airframe designed at NASA Ames Research Center is enlisted for the PAI study. When optimized airframe coupled with the current propulsor designs, the tip circumferential distortion is found higher than the baseline airframe. Nevertheless, the VF fan which is superior in tip pumping pulls off the propulsor efficiency as high as in other configurations while the HSF got a significant performance deficit.

Performance Metrics	VF	HSF
Form Factor	1.95	1.91
MFR (kg/sec)	141	144
Thrust (kN)	10.2	10.68
Propulsive power (kW)	1857.9	1981.8
Shaft power (kW)	2693.6	2972.1
Propulsive Efficiency	1.27	1.25
Propulsor Efficiency (%)	87.7	83.3

Table 3. Performance Comparison of fan/EGV configurations (Type 2 flowpath integrated with the NASA Ames Research Center distortion minimized airframe [22], 37,000 ft., N=2500 RPM)

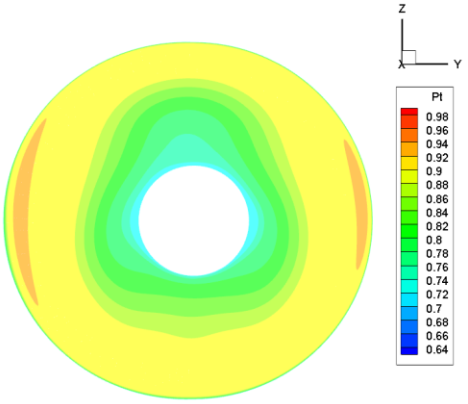

(a) Distortion Minimized (multi-point) Airframe[22]

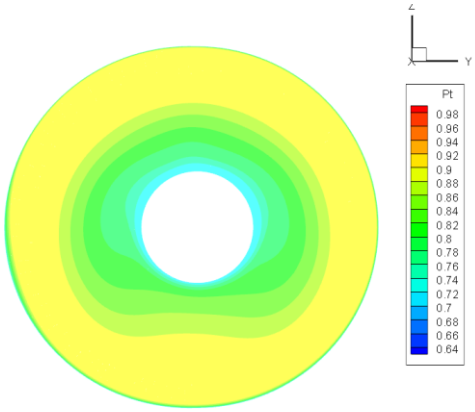

(b) Baseline Airframe

Figure 17. Fan face total pressure contour of distortion minimized airframe and baseline (AOA = 2.0 deg., N= 2500RPM, altitude 37,000ft)

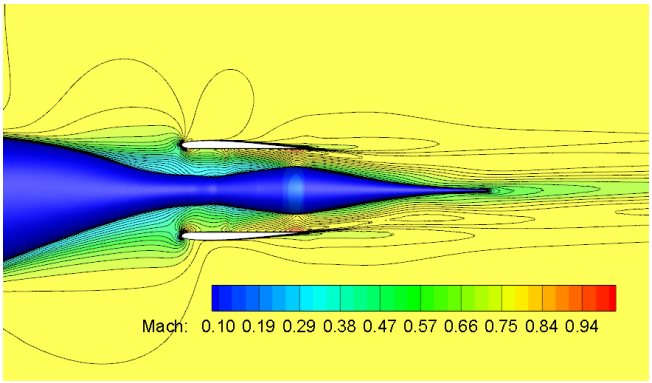

(a) HSF (MFR=145kg/sec)

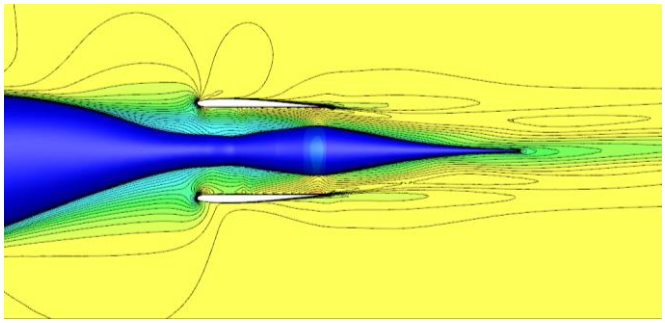

(b) VF (MFR=141kg/sec)

Figure 18. Airframe Integration with (a) HSF, (b) VF propulsors in RANS CFD analysis. (N= 2500RPM, altitude 37,000ft)

ACKNOWLEDGMENTS

In memory of the late Dr. Meng-Sing Liou, the authors sincerely appreciate our co-author and like to honor his passion and dedication to the development of the next generation subsonic fixed wing aircraft with boundary layer ingestion propulsion. We also appreciate financial support of NASA's AATT project and Dr. William Haller, the technical lead of the project. Special thanks to Dr. Mark Celestina (UPAI propulsion technical lead) for the discussion of the direction of propulsor design, Dr. Christopher Hughes (AATT UPAI sub-project manager) for the project support, Dr. Jason Welstead (TCT PI) for airframe integration of STARC-ABL and Mr. Richard Mulac for the technical support of APNASA.

REFERENCES

Smith, L. H., "Wake Ingestion Propulsion Benefit," J. Propulsion and Power, Vol. 9, 74-82, 1993.

[2] Felder, J., Kim, H. D., and Brown, G. V., "An Examination of the Effects of Boundary Layer Ingestion on Turboelectric Distributed Propulsion Systems," AIAA–2011–300, AIAA, 2011.

[3] Lee, B.J., Liou, M.S. and Kim, C., "Optimizing a Boundary-Layer-Ingestion Offset Inlet by Discrete Adjoint Approach," AIAA J. Vol. 48, 2010, doi: 10.2514/1.J050222

[4] Florea, R.V., Voytovych, D., Tillman, G., Stucky, M., Shabbir, A., Sharma, O., and Arend, D., "Aerodynamic Analysis of a Boundary-Layer-Ingesting Distortion-Tolerant Fan," Proceedings of ASME Turbo Expo 2013, San Antonio Texas, GT2013-94656, June 2013.

[5] Cousins, W.T., Voytovch, D. and Tillman, G., "Design of a Distortion-Tolerant Fan for a Boundary-Layer Ingesting Embedded Engine Application," AIAA 2017-5042, 53rd AIAA/SAE/ASEE Joint Propulsion Conference, 10-12 July 2017, Atlanta, GA

[6] Arend, D., Wolter, J.D., Hirt, S.M., Provenza, A.J., Gazzaniga, J.A., Cousins, W.T., Hardin, L.W., and Sharma, O.P., "Experimental Evaluation of an Embedded Boundary Layer Ingesting Propulsor for Highly Efficient Subsonic Cruise Aircraft," AIAA 2017-5041, 53rd AIAA/SAE/ASEE Joint Propulsion Conference, 10-12 July 2017, Atlanta, GA

[7] J. R. Welstead and J. L. Felder, "Conceptual Design of a Single-Aisle Turboelectric Commercial Transport with Fuselage Boundary Layer Ingestion," AIAA-2016-1027, 54th AIAA Aerospace Sciences Meeting, San Diego, California, 2016.

[8] Drela, M., "Development of the D8 Transport Configuration," AIAA2011-3970, 29th AIAA Applied Aerodynamics Conference, 27–30 June 2011, Honolulu, HI.

[9] Hall, D.K., Huang, A.C., Uranga, A., Creitzer, E.M., Drela, M., and Sato, Sho, "Boundary Layer Ingestion Propulsion Benefit for Transport Aircraft," J. Propulsion and Power, Vol. 33, No. 5, September-October 2017.

[10] Liou, M.F., Kim, H.J., B.J.Lee, and Liou, M.S., "Aerodynamic Design of Integrated Propulsion-Airframe Configuration of the Hybrid Wingbody Aircraft," AIAA 2017-3411, 35th AIAA Applied Aerodynamics Conference, 05-09, 2017, Denver, Co, 10.2514/6.2017-3411

[11] Kim, H.J., Liou, M.-F. and Liou, M.-S. "Mail-Slot Nacelle Shape Design for N3-X Hybrid Wing Body Configuration," AIAA 2015-3805, AIAA Propulsion & Energy Forum 2015, Orlando, FL, 27-29 July 2015.

[12] Jones, S.M., "Development of an Object-Oriented Turbomachinery Analysis Code within the NPSS Framework," NASA/TM-2014-216621

[13] Aungier, R.H., "Axial-Flow Compressors: A Strategy for Aerodynamic Design and Analysis," NEW YORK ASME PRESS 2003, ISBN-13: 978-0791801925

[14] Adamczyk, J., Celestina, M., and Beach, T., "Simulation of 3-D Viscous Flow Within a Multi-Stage Turbine, " 34th International Gas Turbine and Aeroengine Congress and Exposition, Toronto, Canada, June 4-8, 1989.

[15] Chima, R. V., "Rapid Calculations of Three-Dimensional Inlet/Fan Interaction," NASA Fundamental Aeronautics 2007 Annual Meeting, New Orleans, LA, Oct. 30–Nov. 1, 2007.

[16] A.Arntz, O. Atinault, D. Destarac, and A. Merlen, "Exergy-based Aircraft Aeropropulsive Performance Assessment: CFD Application to Boundary Layer Ingestion," AIAA 2014-2573, 32nd AIAA Applied Aerodynamics Conference, AIAA AVIATION Forum, https://doi.org/10.2514/6.2014-2573.

[17] Hughes, C. E., "Aerodynamic Performance of Scale-Model Turbofan Outlet Guide Vanes Designed for Low Noise, " AIAA-2002-0374, AIAA, 2002. Also NASA/TM-2001-211352, 2011.

[18] König, W. M., Hennecke, D. K., and Fottner, L., "Improved Blade Profile Loss and Deviation Angle Models for Advanced Transonic Compressor Bladings: Part I-A Model for Subsonic Flow, and Part II-A Model for Supersonic Flow," J. of Turbomachinery, Vol 118, Issue 1, pg. 73-87, Jan 1996.

[19] Deb, K. Agrawal, S., Pratap, A., Meyarivan, T., "A Fast and Elitist multi-objective Genetic Algorithm: NSGA-II," IEEE Transactions on Evolutionary Computation (IEEE-TEC), Vol.6, No.2, pp.182-197, 2002.

[20] Gong, Y., A, "Computational Model for Rotating Stall Inception and Inlet Distortion in Multistage Compressors," Ph.D. Dissertation, Massachusetts Institute of Technology, Dept of Aeronautics and Astronautics, 1998.

[21] Kim, H.J., and Liou, M.-S. "Flow simulation and optimal shape design of N3-X hybrid wing body configuration using a body force method," Aerospace Science and Technology, Oct. 2017.

[22] Kenway, Gaetan, Cadieux, F. and Kiris, C. "Aerodynamic shape optimization of the STARC-ABL concept for minimal inlet distortion," submitted to AIAA SciTech 2018.